Discovery of an essential mycobacterial polar growth factor involved in cell envelope integrity and LM/LAM transport

Kuldeepkumar R. Gupta[a], Kathryn C. Rahlwes[b], Chunyan Wang[c], Jun Liu[c], Yasu S. Morita[b], and E. Hesper Rego[a,1]

[a]Department of Microbial Pathogenesis, Yale University School of Medicine, New Haven, CT 06519

[b]Department of Microbiology, University of Massachusetts, Amherst, MA 01003

[c]Department of Microbial Pathogenesis, Microbial Sciences Institute, Yale School of Medicine, New Haven, CT, USA 06519

[1]To whom correspondence should be addressed: hesper.rego@yale.edu

ABSTRACT. Mycobacteria grow and divide differently compared to well-studied model bacteria. They insert new cell envelope at their poles instead of along their side walls; and, they lack obvious homologs of well-conserved cell growth and division proteins. Furthermore, while mycobacteria are classified as Gram-positive, unlike other bacteria in this taxon, they possess an outer membrane abundant in long-chain fatty acids and several glycolipids. A better understanding of the unique factors that make this unusual structure could lead to therapeutic targets for pathogenic mycobacteria. Here, we study a gene of previously unknown function - *msmeg_0317* - predicted to be essential and associated with mycobacterial cell growth and division proteins. We find that transcriptional depletion of *msmeg_0317* leads to loss of polar growth, disruption of the outer mycobacterial cell wall, and cell death. Surprisingly, we also observe that depletion

results in the accumulation of glycolipids lipomannan and lipoarabinomannan (LM/LAM) in the periplasm. LM/LAM have been extensively studied in relation to infection but their role in bacterial physiology is less clear. Altogether, our data suggest that MSMEG_0317, renamed CwdA, is involved in the transport of LM/LAM to the mycobacterial surface, and reveal unexpected connections between the correct localization of LM/LAM, polar growth, and the structural integrity of the mycobacterial cell envelope.

Introduction

Mycobacterium tuberculosis (Mtb), the agent of human tuberculosis (TB), is responsible for approximately 1.5 million deaths each year. One of the pathogen's distinguishing features is its unusual cell envelope. Like nearly all other bacterial species, the plasma membrane is surrounded by peptidoglycan, a rigid mesh-like structure made up of sugars and peptides. However, in contrast to the peptidoglycan of other well-characterized bacteria, mycobacterial peptidoglycan is covalently linked to the highly branched hetero-polysaccharide arabinogalactan, which is, itself, covalently bound to extremely long chained fatty acids called mycolic acids. In addition to this core structure, several lipids and glycolipids, are abundantly and non-covalently interspersed across the plasma membrane and mycobacterial cell wall (1, 2). This multi-laminate cell envelope is a double-edged sword: it is a formidable barrier to many antibiotics, yet provides a number of potentially targetable structures. Indeed, two, of the four, first-line TB antibiotics target cell-wall biosynthesis.

In addition to its unusual cell envelope, mycobacterial physiology is distinctly different than other model bacterial species. Notably, mycobacteria elongate from their

47 poles rather than along their side walls. The details of polar growth are poorly understood
48 (3-5). Many key proteins important for cell elongation in other species appear to be
49 missing in mycobacteria (4, 6). Likewise, it is almost completely unknown how proteins
50 involved in synthesizing the different layers, and free (glyco)lipids, work together to build
51 the complex cell envelope.

52 Given its unusual physiology, perhaps it is unsurprising that greater than 25% of
53 the mycobacterial genome encodes genes of unknown function (7). In our previous
54 studies on the mycobacterial division complex, 'the divisome', we precipitated known
55 divisome and elongasome components from *M. smegmatis* (Msm), and identified multiple
56 candidate mycobacterial-specific divisome proteins in the precipitate, (6, 8). One of these
57 was MSMEG_0317, a protein of unknown function that is highly conserved in
58 actinobacteria. The Mtb homolog of *msmeg_0317*, *rv0227c*, is predicted to be essential
59 (9, 10). Here, as we sought to understand the role of MSMEG_0317 during mycobacterial
60 growth and division.

61 MSMEG_0317 belongs to the DUF3068-domain super-family of proteins, which
62 are exclusively found in actinobacteria. One member of this family in corynebacteria has
63 channel activity, so this domain has been renamed PorA (11). In addition, by structure-
64 based homology prediction, MSMEG_0317 shares limited homology to mycobacterial
65 lipoproteins, LppX and LprG, which transport lipids, PDIM and TAG, respectively, to the
66 outer mycobacterial cell wall (12, 13).

67 We find that MSMEG_0317 localizes to sites of new cell wall synthesis and is
68 indeed essential for cell viability in Msm. Transcriptional depletion leads to loss of cellular
69 elongation, reductive division, and eventually cell lysis. Surprisingly, we find that

70 lipomannan (LM), and lipoarabinomannan (LAM) – two large glycolipids abundant
71 throughout the mycobacterial cell envelope - accumulate as *msmeg_0317* is depleted,
72 and are shed into the culture media more abundantly upon MSMEG_0317
73 overexpression (1, 14). By cryo-electron microscopy, we find that the cell envelopes of
74 depleted cells are devoid of outer cell wall and are highly disrupted. Together, these
75 results show that MSMEG_0317 plays an important role in LM/LAM transport to the outer
76 mycobacterial cell wall, polar elongation, and the structural organization of the
77 mycobacterial cell wall. As such, we propose to rename *msmeg_0317*, *cwdA*, for cell wall
78 disruption, mutant A.
79

80 **Results**

81 ***cwdA* is essential for polar growth and cell wall integrity**

82 To determine the essentiality of *cwdA*, we used an allele swapping strategy (15).
83 Briefly, in a strain of Msm whose only copy of *cwdA* was at the L5 phage integration site
84 (16), we exchanged *cwdA* for either an empty vector or for another copy of itself (Fig. 1A).
85 Consistent with *cwdA* being essential for cell growth, we observed approximately 1000-
86 fold fewer colonies when we exchanged *cwdA* with an empty vector compared to
87 exchanging it for another copy of itself (Fig. 1A).

88 To further confirm the essentially of *cwdA* we constructed a strain in which the only
89 copy of the gene was tetracycline inducible (Fig. 1B). Removal of anhydrotetracycline
90 (ATC) from the culture media prevented cell growth (Fig. 1B). By time-lapse microscopy
91 we observed that, while cells expressing *cwdA* became longer, on average, as cell density
92 increased within the microfluidic device (Fig. 2A, C & Movie S1), cells depleted for *cwdA*

93 stopped elongating but continued to divide (reductive division), became wider, and, in
94 many instances, eventually lysed (Fig. 2B,C & Movie S2). Together these data show that
95 *cwdA* is essential for polar elongation in Msm.
96
97 **CwdA localizes to the sites of cell wall synthesis**
98 As our data suggested CwdA is important for polar growth, we hypothesized that
99 it would localize to the poles, which are the site of new cell wall synthesis in mycobacteria.
100 To test this hypothesis, we made a translational fusion to CwdA with mRFP expressed by
101 its native promoter. By allele swapping, we find that *cwdA-mrfp* restores bacterial growth
102 (Fig. S1) and thus encodes a functional *cwdA*. Fluorescence microscopy at a single time-
103 point showed that CwdA-mRFP localizes to mid-cell and to the poles (Fig. 3A). In polar
104 growing bacteria, the site of division eventually becomes the site of elongation. Thus, in
105 addition to localizing to the poles, elongation-complex proteins will also localize to the site
106 of division early during the cell cycle. To disentangle whether CwdA is also part of the
107 division complex we visualized CwdA-mRFP by time-lapse microscopy. By constructing
108 kymographs averaged over many cells, we compared the fluorescence distribution over
109 the course of the cell cycle to the earliest known marker for the division (FtsZ-mCherry2B)
110 complex and the elongation complex (eGFP-Wag31). CwdA-mRFP localizes to the site
111 of division after FtsZ (Fig. 3A, B), but before Wag31 (Fig. 3C). These data are consistent
112 with CwdA being a member of both the mycobacterial division and elongation complexes,
113 but its essential function is as part of the elongation complex.
114
115 **CwdA is involved in LM/LAM transport and cell wall integrity**

116 The corynebacterial homolog of *cwdA* was recently implicated in LM/LAM
117 biosynthesis (17), as a deletion mutant of the *Corynebacterium glutamicum* homolog
118 results in truncated LM. To test if this is also the case in mycobacteria we used thin layer
119 chromatography (TLC) to quantify the amounts of different lipid species in cells depleted
120 for CwdA. In contrast to the results obtained in *C. glutamic*, we observe a dramatic
121 increase in the total amount of cell-associated of LM/LAM during depletion (Fig. 4A), while
122 other lipids (Fig. 4 B, C & Fig. S4) and sugars (Fig. S2) remain constant. Likewise, when
123 we inducible over-expressed *cwdA* from a multicity plasmid, we observed less LM/LAM
124 associated with Msm cells (Fig. S3A & S5).

125 These data are not consistent with the proposed function of the corynebacteria
126 *cwdA* homolog. As, by sequence-based homology modeling, CwdA shares some
127 homology to Lapps and PGR, proteins known to transport lipids from the inner membrane
128 to the outer membrane in mycobacteria, we hypothesized that CwdA could be involved in
129 transporting LM/LAM to the outer membrane where it is likely to be shed (18-20).
130 Consistent with this hypothesis, upon over-expression of CwdA we observed more
131 LM/LAM in the culture supernatant (Fig. S3B). These data show that that CwdA is
132 involved in transporting LM/LAM to the cell surface of mycobacteria (Fig. S3B).

133

134 **CwdA is important for outer cell wall integrity.**

135 Given the abrupt and violent nature of lysis when cells are depleted for CwdA, we
136 hypothesized that CwdA-depleted cells had gross alterations to their cell envelope. Thus,
137 we visualized the cell envelope of wild type and mutant cells by high resolution cryo-
138 electron microscopy (cryo-EM). As has been previously observed (21, 22), wild type Msm

139 cells exhibit a distinct plasma membrane and outer membrane that is approximately 50-
140 nm thick (Fig. 5A-C). Surprisingly, we find that cells depleted for CwdA have largely
141 unstructured cell walls, and appear devoid of electron density in the outer cell wall (Fig. 5
142 D-F). Early during depletion, before cell death, we observe dramatic fraying of the outer
143 membrane, and large invaginations of plasma membrane (Fig. 6). Thus, CwdA is
144 important for maintaining the structural integrity of the outer mycobacterial cell wall.

145 Collectively, our data show that CwdA is an essential polar growth factor involved
146 in transporting LM/LAM to the outer wall. Further, our data suggest that the correct
147 localization of LM/LAM is important for the structural organization and integrity of the
148 mycobacterial cell envelope.

149

150 **Discussion**

151 The extraordinary diversity of the bacterial kingdom has led to a plethora of
152 bacterial cell shapes and geometries of cell growth and division. Unlike well-studied
153 model bacteria, several organisms, including the major human pathogen *Mycobacterium*
154 *tuberculosis,* grow from their poles rather than their side-walls. Our understanding of polar
155 growth is at a nascent stage compared to our knowledge of side-wall growth.
156 Mycobacteria, and related organisms, have an additional challenge of orchestrating the
157 biosynthesis and transport of several additional covalently and non-covalently attached
158 lipids and sugars to their thick layer of peptidoglycan. How these organisms coordinate
159 the biogenesis of this complex structure to elongate and divide is almost completely
160 unknown.

161 Here, we have identified a highly conserved actinobacteria protein, MSMEG_0317,
162 in *M. smegmatis* and propose to rename it CwdA. We show that this gene is essential in
163 Msm. The Mtb homolog, *rv0227c*, is almost certainly essential as well, as no transposon
164 insertions have been found in this gene, even in data sets which combine insertion counts
165 from high density mutagenesis across multiple independent experiments (9).

166 Our data suggest that Wad's essential function occurs during polar elongation, as
167 cells depleted for CwdA stop elongating, and CwdA-mRFP localizes to the poles.
168 Interestingly, CwdA also localizes to the site of division, yet depleted cells continue to
169 divide. This is consistent with recent work from several groups, which suggests that the
170 essentiality of certain cell envelope structures is different for elongation and division. For
171 example, *C. glutamic* cells treated with ethambutol, which inhibits the polymerization of
172 Arabian, a core structure in both arabinogalactan and LAM, stop elongating, but continue
173 to divide (23, 24).

174 What is the function of CwdA? Our work suggests that CwdA is involved in the
175 transport of LM/LAM to the cell surface either directly or indirectly, and for maintaining the
176 structural integrity of that mycobacterial cell wall. Upon depletion, the levels of several
177 other lipids remain constant, suggesting that *cwdA* may be acting on LM/LAM directly,
178 though our lipid profiling was not exhaustive and we cannot rule out the possibility that
179 another structural lipid is affected by CwdA depletion. However, supporting the notion that
180 CwdA specifically acts upon LM/LAM, we observe a temporal correlation, up until the time
181 of cell lysis, between the accumulation of LM/LAM and the disruption of the envelope.
182 This leads the question: Could LM/LAM be essential components of the outer cell
183 envelope? There has been a good deal of speculation as to the localization of LM/LAM in

184 the mycobacterial envelope, but several groups have now shown that at least a fraction
185 of LM/LAM resides in the outer cell wall (19, 20). Our data are consistent with this model.
186 In addition, our data suggest that either LM/LAM are important structural components of
187 the outer cell wall or the accumulation of these large glycolipids in the periplasm leads to
188 envelope disruption.

189 One implication from our work is that the transport of lipids to the cell surface is
190 needed for polar elongation, but not division, suggesting that there could be various
191 feedback loops to ensure complete construction of the elaborate mycobacterial cell
192 envelope for insertion of new material to elongate. These checkpoints appear missing
193 during division. This notion is supported by other mutants defective in transporting
194 important cell wall components like treehouse monocycle, which, like the *cwdA* mutant,
195 undergo reductive cell division (25).

196 The mycobacterial cell envelope remains an enduring target for the development
197 of new TB therapeutics. The standard TB therapy uses a combination of four drugs; two
198 of these drugs target cell wall synthesis. In addition to the core, and covalently linked
199 structure of peptidoglycan, arabinogalactan, and mycolic acids, the mycobacterial cell
200 envelope is also rich with many other lipids. The functional role of these lipids in bacterial
201 cell physiology is relatively unexplored but they are likely important, if not essential,
202 components of the cell envelope. Our data argue that a more complete understanding of
203 the transport of these molecules could lead to new targets for the development of anti-TB
204 therapeutics.

205

206 **Materials and Methods**

207 **Bacterial strains and culture conditions**: *M. smegmatis* mc^2155 was grown in
208 Middlebrooks 7H9 broth supplemented with 0.05% Tween80, 0.2% glycerol, 5 gm/L
209 albumins, 2 gm/L dextrose and 0.003 gm/L catalase or plated on LB agar. *Escherichia*
210 *coli* DH5α cells were grown in LB broth or on LB agar plates. Concentrations of antibiotics
211 used for *M. smegmatis* is as follows: 20 μg/ml eosin, 25 μg/ml kanamycin, 50 μg/ml
212 hydrolyzing, and 20 μg/ml nourseothricin. Concentrations of antibiotics used for *E. coli*
213 used for E. coli is as follows: 40 μg/ml eosin, 50 μg/ml kanamycin, 100 μg/ml hydrolyzing,
214 and 40 μg/ml nourseothricin.

215 **Plasmids and strains construction:** Before deleting the native copy of
216 *msmeg_0317/cwdA*, a merodiploid strain was created by inserting a second copy of
217 *msmeg_0317/cwdA* gene under pTetO promoter using a Kan^{nur} L5 integrating vector.
218 Subsequently, in the merodiploid strain, an in-frame deletion was made by replacing the
219 native copy of *msmeg_0317/cwdA gene* with a eosin resistance cassette flanked by lox
220 sites using recombineering (16). The plasmid constructs were made using isothermal
221 Gibson assembly whereby insert and vector backbone shared 20-25 bp of homology.
222 *msmeg_0317/cwdA* and its fluorescent variant were cloned in a Nat L5 integrating vector
223 for allele exchange at L5 site. The *msmeg_0317/cwdA* depletion strain was made by
224 transforming an episomally Her marked vector constitutively expressing Tetra repressor
225 into a strain expressing *msmeg_0317* gene under pTetO promoter. mRFP was fused to
226 the c-terminal of *msmeg_0317* gene cloned with 200 bp upstream sequence to capture
227 the native promoter. *ftsZ-mCherry*2B and *eGFP-wag31* genes were cloned under medium
228 strength promoter ptb21 and integrated at tweedy (two) and L5 phage integration sites,
229 respectively.

230 **MSMEG_0317 Depletion:** To transcriptionally deplete *msmeg_0317/cwdA* in *M.*
231 *smegmatis*, anhydrotetracycline-inducible Tet-ON system was used. The
232 *msmeg_0317/cwdA* gene was expressed from pTetO promoter, while the TetR repressor
233 was constitutively expressed in trans from an episomal vector. MSMEG_0317 was
234 depleted by removing anhydrotetracyline from the medium and cells were grown for 18
235 hours. Subsequently, MSMEG_0317 cells depleted cells were re-diluted in fresh medium.
236 Alternatively, depletion was achieved by removing and adding fresh medium every three
237 hours from 18hr-old depletion cultures.

238 **Time-lapse microscopy**: An inverted Nikon Ti-E microscope was used for the
239 time-lapse imaging. An environmental chamber was maintained at 37°C. Cells were
240 cultivated in an B04 microfluidics plate from CellAsic; continuously supplied with fresh
241 medium; and imaged every 15 minutes using phase contrast.

242 **Kymograph analysis.** Time-lapse images were analyzed in open source image
243 analysis software Fiji (26) and a custom MATLAB program was used to generate
244 kymographs. Specifically, for a single cell, in Fiji, a 5-pixel wide segmented line was drawn
245 from the new pole to the old pole at each time point during the cell cycle. This was
246 repeated on 20-50 cells. These line profiles were then imported into Matlab, where a
247 custom script was used to generate an average kymograph by 2D interpolation of the
248 individual kymographs.

249 **Lipid extraction and analysis.** Crude lipids were extracted from the
250 MSMEG_0317*/cwdA* depletion strains after 18, 24, 27, 30, and 33 hrs without
251 anhydrotetracycline, following a previously published protocol(27). Briefly, LM and LAM
252 were extracted from the delipidated pellet by incubation with phenol/water (1:1) for 2 hrs

253 at 55°C. Phospholipids and PIMs were separated by high performance thin layer
254 chromatography (HPTLC) silica gel 60 (EMD Merck) using chloroform/methanol/ 13M
255 ammonia/1M ammonium acetate/ water (180:140:9:9:23). Phospholipids were visualized
256 via cupric acetate staining. Carbohydrates extracted in the aqueous phase of the butanol-
257 water phase partitioning were separated by HPTLC using the solvent n-butanol/
258 isoproponal/ water (13:12:4). GPLs were separated using the solvent chloroform/
259 methanol/ water (90:10:1). GPLs, carbohydrates and PIMs were visualized with orcinol
260 staining as described (Sena 2010). LM/LAM samples were separated by SDS-PAGE
261 (15% gel) and visualized using ProQ Emerald 488 glycan staining kit (Life Technologies)
262 as described in (28). To detect LM/LAM in culture supernatants, the supernatants were
263 initially treated with a final concentration of 50 μg/ml Proteinase K for 4 hours at 50°C.
264 The treated supernatants were electrophoresed on 15% SDS-PAGE. LM/LAM were
265 blotted onto nitrocellulose at 20 V for 45 minutes using semi-dry transfer method. Post-
266 transfer, the membrane was blocked by 5% milk. The blocked membrane was then
267 probed with CS-35 antibody (BEI Resources, NIH) at 1:250 dilution at 4°C overnight. The
268 membrane was washed with 1X TBST five times for five minutes each. Post-washing, it
269 was probed with anti-mouse secondary for one hour at room temperature. Membrane
270 was then washed five times for five minutes with 1X TBST. Thermo Scientific's west dura
271 chemiluminescent reagent was used to develop the membrane.

272 **Sample preparation and image collection for Cryo-EM:** Wild type and
273 MSMEG_0317/CwdA depleted Msm were pelleted, washed twice with 1X phosphate
274 buffered saline (PBS), and suspended in a very small volume of PBS to get a very dense
275 suspension of bacterial cells. The dense culture was subsequently mixed with 10-nm

colloidal gold and deposited onto fresh glow-discharged holey carbon grids. The grids were then blotted with filter paper manually and rapidly frozen in liquid ethane. The frozen grids were transferred under -170 °C into a 300kV Titan Krios equipped with K2 Summit direct detector, a quantum energy filter (Gatan, Pleasanton, CA) and an FEI volta phase plate (FEI). The data was collected using SerialEM (29) and Digital Micrograph softwares. The motion correction for each movie was done with MotionCor2 (30). The microscope was operated at 300kV with a magnification of 3,600x and 26,000 x for low-mag map and high-mag map respectively. The grey levels of each micrograph are obtained using MatLab.

Acknowledgements

We thank Cara Boutte and Maikel Boot for helpful suggestions and for critical reading of the manuscript. Work carried out in this manuscript was supported by career award at scientific interface (CASI) from Burroughs Welcome Fund and Searle and Pew funds to E.H.R.

References:

1. Jackson M (2014) The mycobacterial cell envelope-lipids. *Cold Spring Harb Perspect Med* 4(10).
2. Jankute M, Cox JA, Harrison J, & Besra GS (2015) Assembly of the Mycobacterial Cell Wall. *Annu Rev Microbiol* 69:405-423.
3. Kieser KJ & Rubin EJ (2014) How sisters grow apart: mycobacterial growth and division. *Nat Rev Microbiol* 12(8):550-562.
4. Hett EC & Rubin EJ (2008) Bacterial growth and cell division: a mycobacterial perspective. *Microbiol Mol Biol Rev* 72(1):126-156, table of contents.
5. Baranowski C, Rego EH, & Rubin EJ (2019) The Dream of a Mycobacterium. *Microbiology spectrum* 7(2).

304 6. Wu KJ, *et al.* (2018) Characterization of Conserved and Novel Septal Factors in
305 Mycobacterium smegmatis. *J Bacteriol* 200(6).
306 7. Doerks T, van Noort V, Minguez P, & Bork P (2012) Annotation of the M. tuberculosis
307 hypothetical orfeome: adding functional information to more than half of the
308 uncharacterized proteins. *PLoS One* 7(4):e34302.
309 8. Rego EH, Audette RE, & Rubin EJ (2017) Deletion of a mycobacterial divisome factor
310 collapses single-cell phenotypic heterogeneity. *Nature* 546(7656):153-157.
311 9. DeJesus MA, *et al.* (2017) Comprehensive Essentiality Analysis of the Mycobacterium
312 tuberculosis Genome via Saturating Transposon Mutagenesis. *mBio* 8(1).
313 10. Zhang YJ, *et al.* (2012) Global assessment of genomic regions required for growth in
314 Mycobacterium tuberculosis. *PLoS Pathog* 8(9):e1002946.
315 11. Soltan Mohammadi N, *et al.* (2013) Identification and characterization of the channel-
316 forming protein in the cell wall of Corynebacterium amycolatum. *Biochimica et biophysica*
317 *acta* 1828(11):2574-2582.
318 12. Sulzenbacher G, *et al.* (2006) LppX is a lipoprotein required for the translocation of
319 phthiocerol dimycocerosates to the surface of Mycobacterium tuberculosis. *The EMBO*
320 *journal* 25(7):1436-1444.
321 13. Martinot AJ, *et al.* (2016) Mycobacterial Metabolic Syndrome: LprG and Rv1410 Regulate
322 Triacylglyceride Levels, Growth Rate and Virulence in Mycobacterium tuberculosis. *PLoS*
323 *Pathog* 12(1):e1005351.
324 14. Mishra AK, Driessen NN, Appelmelk BJ, & Besra GS (2011) Lipoarabinomannan and
325 related glycoconjugates: structure, biogenesis and role in Mycobacterium tuberculosis
326 physiology and host-pathogen interaction. *FEMS Microbiol Rev* 35(6):1126-1157.
327 15. Pashley CA & Parish T (2003) Efficient switching of mycobacteriophage L5-based
328 integrating plasmids in Mycobacterium tuberculosis. *FEMS Microbiol Lett* 229(2):211-
329 215.
330 16. van Kessel JC & Hatfull GF (2007) Recombineering in Mycobacterium tuberculosis. *Nat*
331 *Methods* 4(2):147-152.
332 17. Cashmore TJ, *et al.* (2017) Identification of a Membrane Protein Required for Lipomannan
333 Maturation and Lipoarabinomannan Synthesis in Corynebacterineae. *J Biol Chem*
334 292(12):4976-4986.
335 18. Pitarque S, *et al.* (2008) The immunomodulatory lipoglycans, lipoarabinomannan and
336 lipomannan, are exposed at the mycobacterial cell surface. *Tuberculosis (Edinburgh,*
337 *Scotland)* 88(6):560-565.
338 19. Gaur RL, *et al.* (2015) Correction: LprG-Mediated Surface Expression of
339 Lipoarabinomannan Is Essential for Virulence of Mycobacterium tuberculosis. *PLoS*
340 *Pathog* 11(12):e1005336.
341 20. Shukla S, *et al.* (2014) Mycobacterium tuberculosis lipoprotein LprG binds
342 lipoarabinomannan and determines its cell envelope localization to control
343 phagolysosomal fusion. *PLoS Pathog* 10(10):e1004471.
344 21. Zuber B, *et al.* (2008) Direct visualization of the outer membrane of mycobacteria and
345 corynebacteria in their native state. *J Bacteriol* 190(16):5672-5680.
346 22. Hoffmann C, Leis A, Niederweis M, Plitzko JM, & Engelhardt H (2008) Disclosure of the
347 mycobacterial outer membrane: cryo-electron tomography and vitreous sections reveal the
348 lipid bilayer structure. *Proc Natl Acad Sci U S A* 105(10):3963-3967.

23. Zhou X, *et al.* (2019) Sequential assembly of the septal cell envelope prior to V snapping in Corynebacterium glutamicum. *Nature chemical biology* 15(3):221-231.
24. Schubert K, *et al.* (2017) The Antituberculosis Drug Ethambutol Selectively Blocks Apical Growth in CMN Group Bacteria. *mBio* 8(1).
25. Fay A, *et al.* (2019) Two accessory proteins govern MmpL3 mycolic acid transport in mycobacteria. *bioRxiv*:581447.
26. Schindelin J, *et al.* (2012) Fiji: an open-source platform for biological-image analysis. *Nat Methods* 9(7):676-682.
27. Sena CB, *et al.* (2010) Controlled expression of branch-forming mannosyltransferase is critical for mycobacterial lipoarabinomannan biosynthesis. *J Biol Chem* 285(18):13326-13336.
28. Rahlwes KC, *et al.* (2017) The cell envelope-associated phospholipid-binding protein LmeA is required for mannan polymerization in mycobacteria. *J Biol Chem* 292(42):17407-17417.
29. Mastronarde DN (2005) Automated electron microscope tomography using robust prediction of specimen movements. *J Struct Biol* 152(1):36-51.
30. Zheng SQ, *et al.* (2017) MotionCor2: anisotropic correction of beam-induced motion for improved cryo-electron microscopy. *Nat Methods* 14(4):331-332.

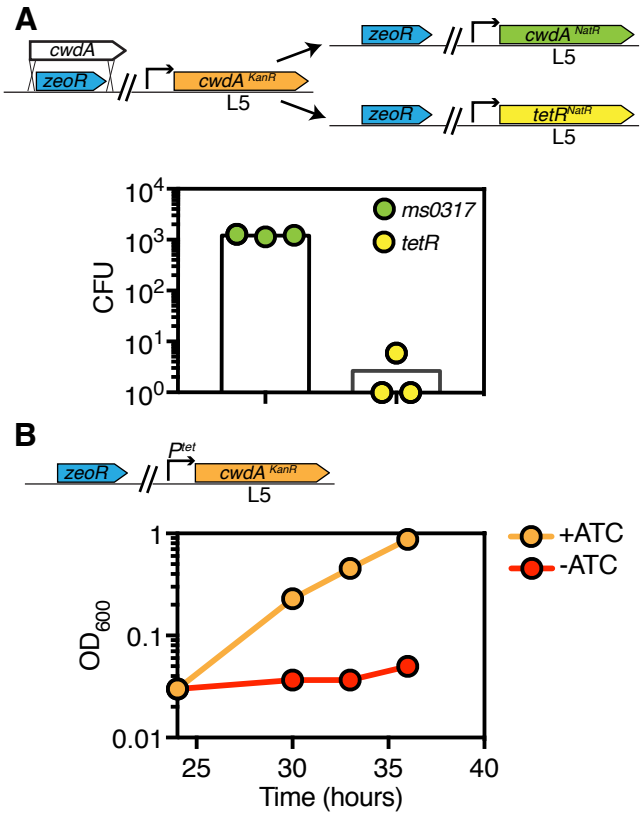

Fig. 1. *cwdA* is essential in *M. smegmatis*. (A) L5-integrating vectors carrying either a copy of *cwdA* or a gene encoding *tetR* were transformed into a strain whose only copy of *cwdA* was at the L5 integration site, and transformants were counted. Bars represent means of biological triplicates and are representative data of 3 independently performed experiments. (B) Optical density over time of a strain whose only copy of *cwdA* is tetracycline inducible (+/-ATC). Points are means of three biological replicates. Error bars are too small to be visible. Experiment was performed at least 4 times on separate days, and representative data are shown. ATC=anhydrotetracycline. Time on the x-axis corresponds to time after ATC was removed.

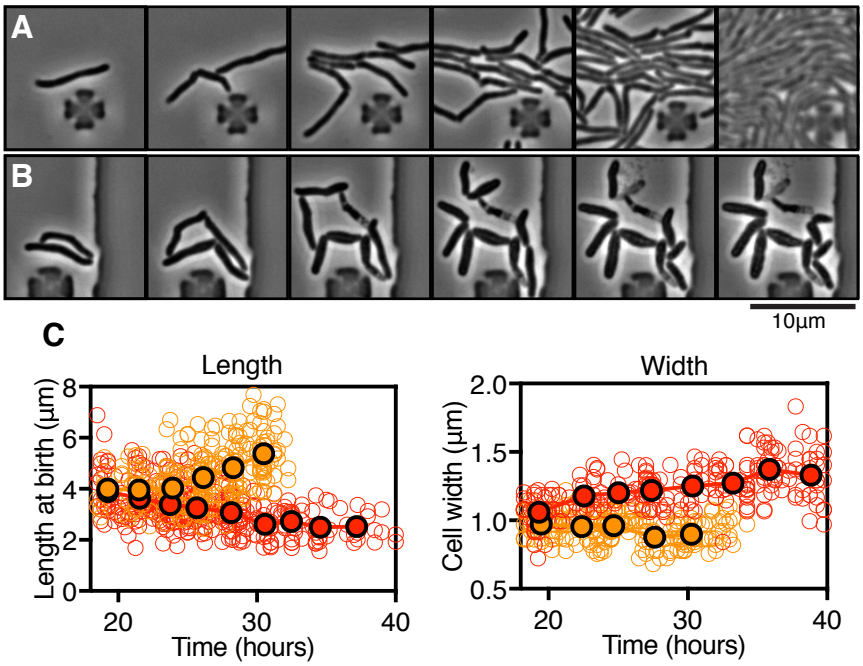

Fig. 2. *cwdA*-depletion causes reductive cell division and eventual cell lysis. (A,B) The strain shown in Fig. 1B was visualized by time-lapse microscopy in the presence (A) or absence of ATC (B). Cells were loaded into a microfluidic device 18 hours after the removal of ATC (B) or a mock control (A). Representative frames are 3 hours apart. (C) Birth lengths and cell widths over time of depletion (orange = +ATC; red = -ATC). Open circles represent individual cells (length: N = 261 (length) & 253 (width) for +ATC; N = 355 (length) & 254 (width) -ATC). Closed circles are not fits to the data but represent the mean of cells in 2.25-hr (length) or 2.75-hr (width) bins. The experiment was performed twice on separate days. In +ATC cultures, cell density became too high to measure length and width past ~33 hrs.

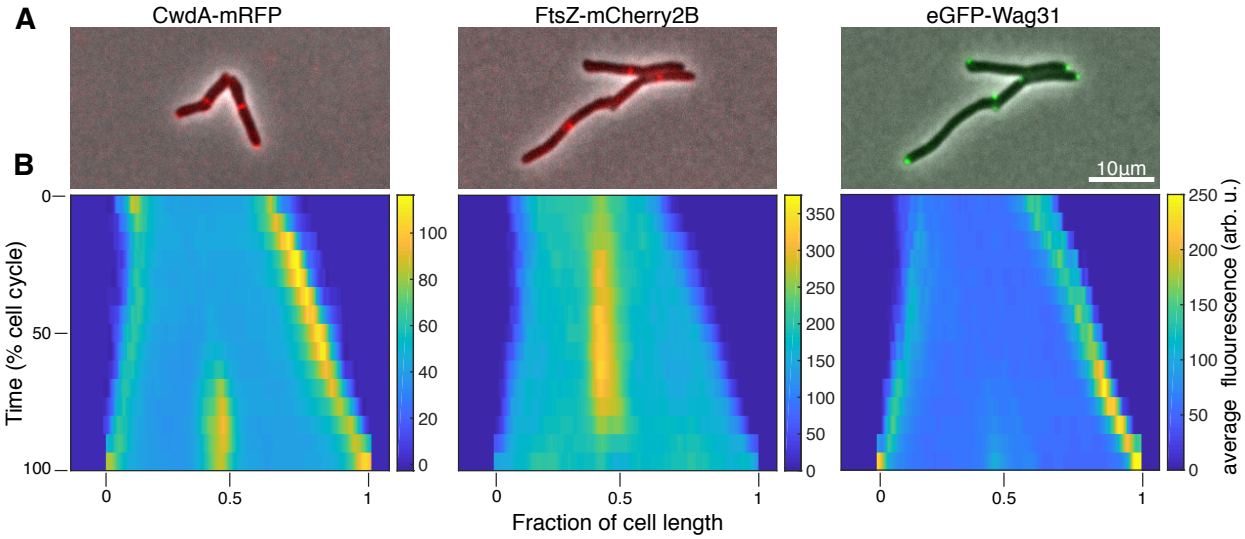

Fig. 3. CwdA localizes to the sites of division and elongaton. (A) Merged phase-contrast and fluorescence images of Msm cells expressing CwdA-mRFP, eGFP-Wag31 and FtsZ-mCherry2b. (B) Average fluorescent distributions over time (kymographs) from cells aligned from new to old poles and from birth to division (N=20 CwdA-mRFP; N=48 FtsZ-mCherry2B; N=20 eGFP-Wag31).

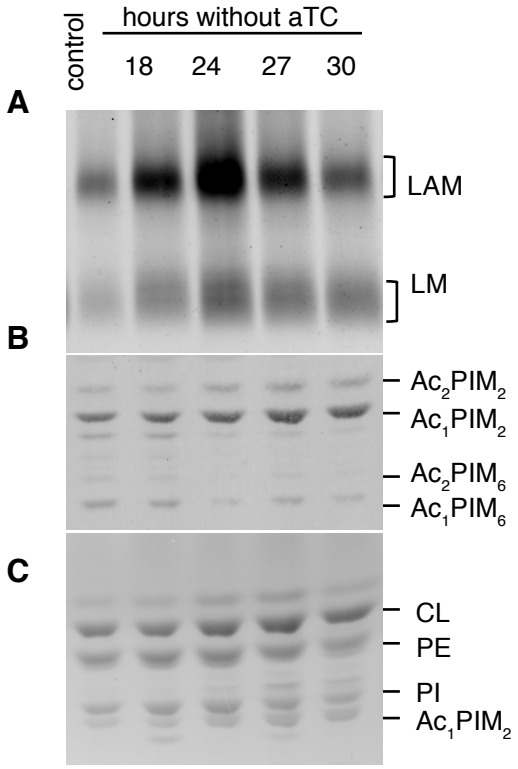

412
413
414 **Fig. 4. LM/LAM accumulate as *cwdA* is depleted**. (A-C) In cells depleted for *cwdA*,
415 LM/LAM are separated by SDS-PAGE (A); non-polar and polar PIMS (B), and plasma-
416 membrane lipids (C) are measured by TLC.
417
418

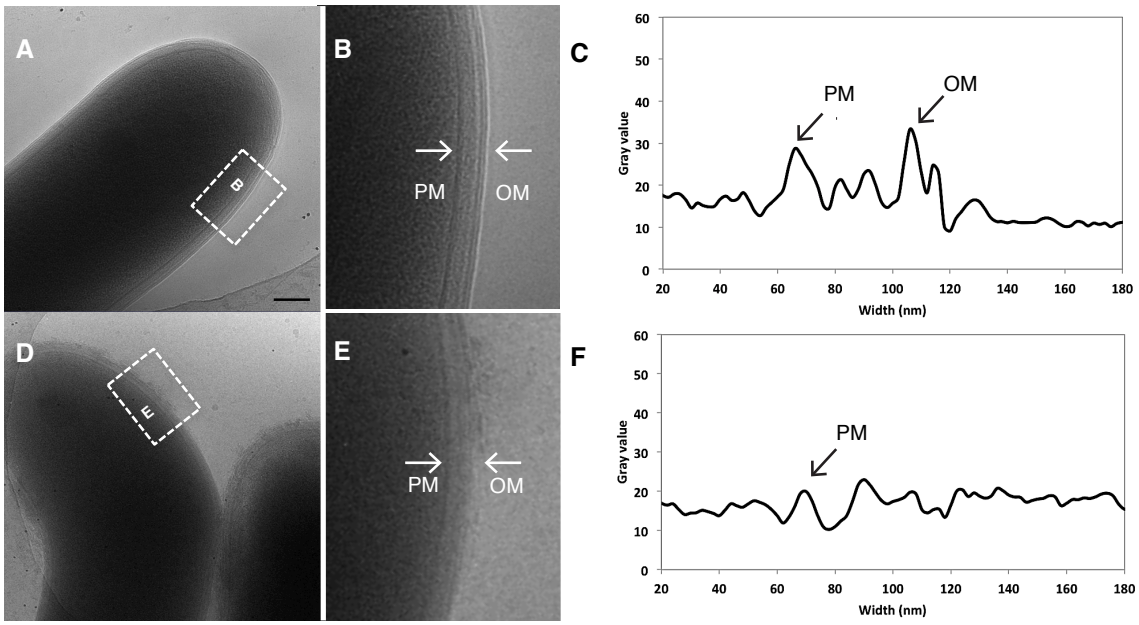

Fig. 5. Depletion of CwdA leads to loss of outer cell wall. The cell envelope of a representative wild type *M. smegmatis* cell (A-C) and a cell depleted for CwdA for 24 hours (D-F) visualized (A,B,D,E) and measured (D,F) by cryo-electron microscopy. PM = plasma membrane; OM = outer membrane.

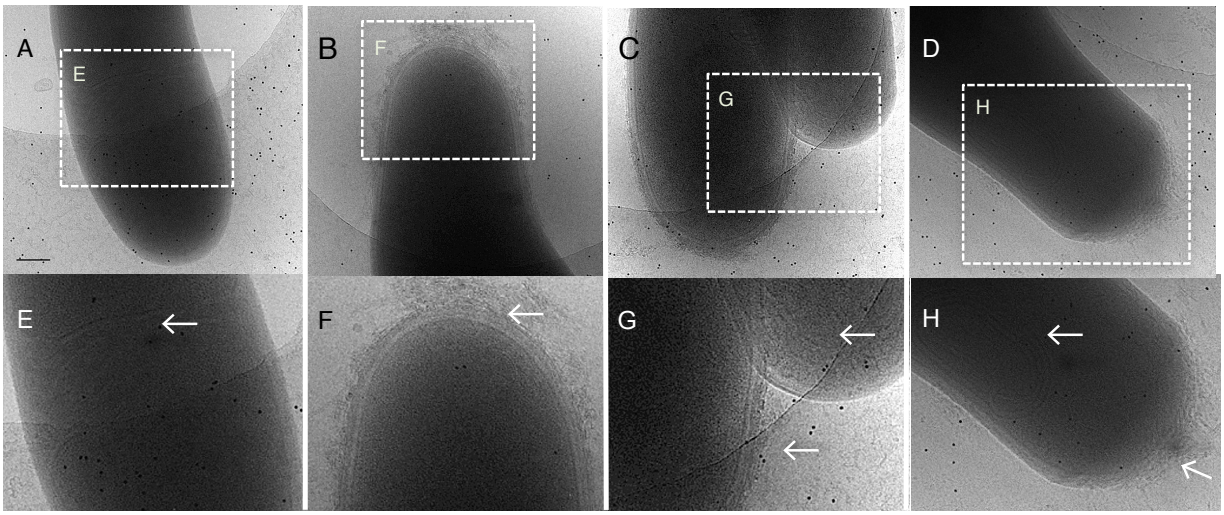

Fig. 6. Cryo-Electron Microscopy of CwdA-depleted cells (A-H) The cell envelopes of CwdA-depleted cells, showing plasma membrane invaginations (A,E,C&H) and outer membrane wall fraying (B-H). (A,E) 24 hrs; (B,F) 24 hrs; (C,G) 24 hrs; (D,H) 33 hrs of depletion.

434 **Supplemental Figures**
435

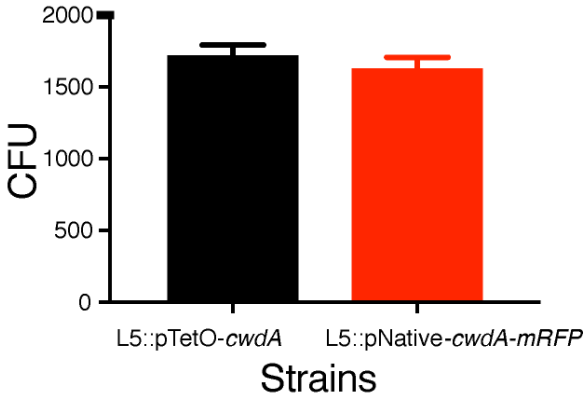

436
437
438 **Fig. S1. CwdA-mRFP encodes a functional copy.** L5-allele swapping with *cwdA* or
439 *cwdA-mRFP* expressed by the native promoter. Bars represent means of 3 biological
440 replicates. Error is standard deviation.
441

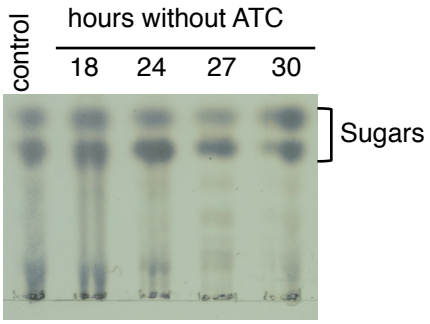

Fig. S2. TLC of unidentified sugars during *cwdA* depletion. This TLC shows that during CwdA depletion the levels of monosaccharides and disaccharides remain constant.

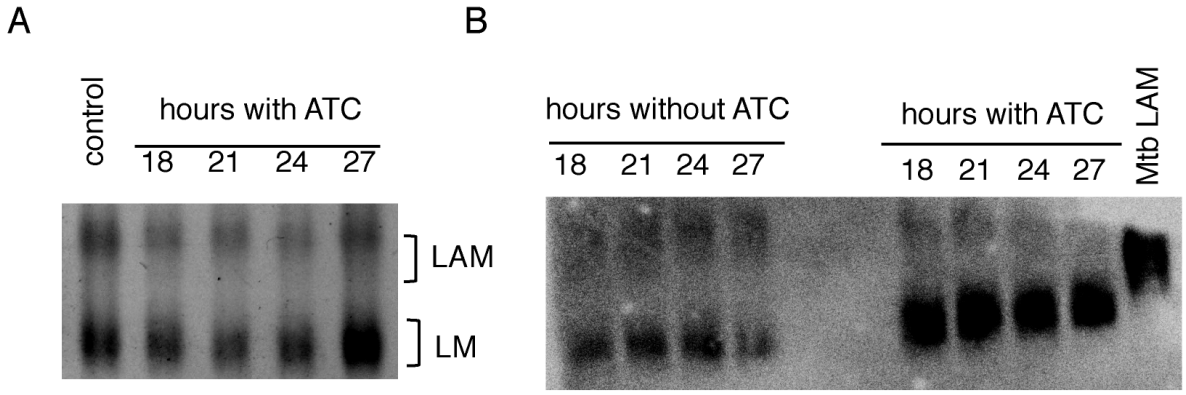

Fig. S3. Detection of LM/LAM during *cwdA* over-expression. A) Detection of cell associated LM/LAM using SDS-PAGE in *cwdA* over-expression. B) Detection of LAM in the culture supernatants using western blot during *cwdA* over-expression using CS-35 antibody. CS-35 antibody is specific to arabinan moiety, hence only LAM is detected in the western blot experiments.

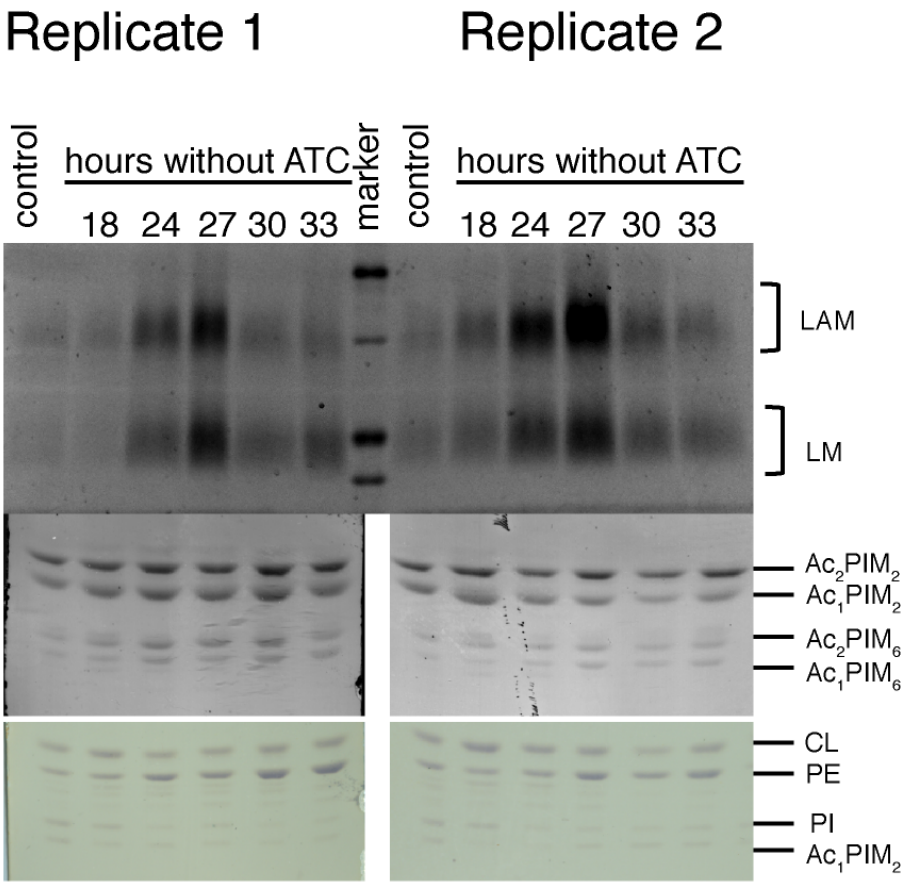

Fig. S3. Accumulation of LM/LAM during *cwdA* depletion. Two independent biological replicates showing that *cwdA* depletion specifically causes an accumulation of LM/LAM before cell death is triggered. Levels of the rest of the cell wall associated lipids remains constant during *cwdA* depletion.

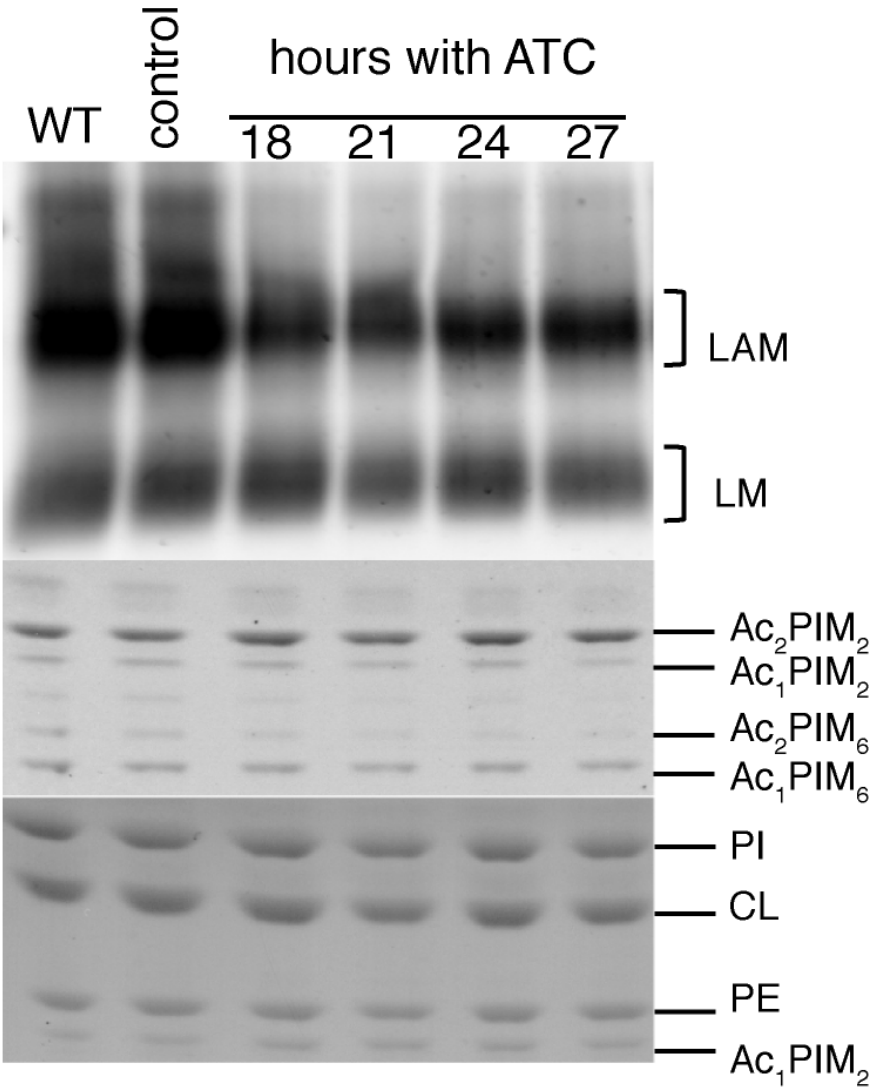

Fig. S5. Detection of cell wall associated lipid during *cwdA* over-expression. LM/LAM levels associated with mycobacterial cells decrease upon *cwdA* over-expression. However, the levels of the rest of the lipids remain constant.